Received: 10 August 2020 | Revised: 24 October 2020 | Accepted: 17 December 2020

DOI: 10.1002/maco.202011997

ARTICLE

Materials and Corrosion

Electrochemical behavior of Zn-REP nanohybrid coatings during marine *Shewanella sp*. biofilm formation

Jonathan J. Calvillo Solís | **Monica Galicia Garcia**

Departamento de Ciencias Químico-Biológicas, Instituto de Ciencias Biomédicas, Universidad Autónoma de Ciudad Juárez, Ciudad Juárez, Chihuahua, México

Correspondence
Monica Galicia Garcia, Departamento de Ciencias Químico-Biológicas, Instituto de Ciencias Biomédicas, Universidad Autónoma de Ciudad Juárez, Ciudad Juárez, CH, México.
Email: monica.galicia@uacj.mx

Abstract

Nanohybrid coatings, particularly zinc-rich epoxy coatings, can protect steel from the harsh marine environment through a physical barrier mechanism and a cathodic protective effect based on anodic electrochemical reactions involving zinc particles in the coating. New additives, such as carbon nanotubes (CNTs), produce more efficient multifunctional coatings by enhancing both protective mechanisms. In this study, the electrochemical behavior and corrosion mechanisms of zinc-rich epoxy nanohybrid coatings with the addition of CNTs were investigated in the presence of a *Shewanella sp*. marine strain to evaluate their influence on biofilm formation by this Gram-negative bacterium. The electrochemical activity was monitored over time with open-circuit potential, electrochemical impedance spectroscopy, and scanning electron microscopy coupled with energy-dispersive X-ray spectroscopy. A mixed mechanism was observed starting from early exposure. When the content of CNTs was doubled, the biofilm adherence improved, thus suggesting a favorable effect of CNTs on biofilm formation, attributable to increased production of bacterial exopolymeric substances facilitating biofilm development. The electrochemical impedance spectroscopy results suggested a correlation with biofilm formation as a second barrier layer with the lowest impedance magnitude in coatings with different multiwalled CNT content.

KEYWORDS

aerobic marine strain, impedance analysis, nanohybrid coatings, *Shewanella sp*., Zn-rich epoxy

1 | INTRODUCTION

Marine biofilm communities are formed when microorganisms adhere to immersed surfaces. These communities have important functions on the surfaces of metallic structures used in industrial infrastructure. A consequence of this settlement is microbiological corrosion, also known as biocorrosion, which can occur in ship hulls, plant cooling systems, pipelines, submerged structures, and oceanographic research instruments, thus resulting in enormous economic losses.[1–3] Studies on the mechanistic aspects of microbiological corrosion on bare steel have focused on anaerobic bacteria, which have been demonstrated to be the organisms most aggressively affecting the corrosion rate, particularly in oil and gas infrastructures under anoxic conditions.[4,5] For carbon steel, some coatings have been designed to provide an effective barrier inhibiting both inorganic corrosion and biocorrosion processes through organic,[6,7] inorganic,[8,9] and hybrid approaches[7,10]; some coatings are environmentally friendly, thus avoiding environmental toxicity due to the use of inherently toxic formulations under aerobic or anaerobic conditions.

Nanohybrid coatings, also called nano-architected sacrificial coatings, have emerged as a new technology with dual protective mechanisms: (a) *Cathodic protection* achieved by the integration of electrochemically active and sacrificial particles into the organic coating matrix, thus resulting in a galvanic effect, and (b) *barrier protection*, physical protection conferred by the polymeric matrix itself. New formulations, including carbon nanotubes (CNTs) in hybrid zinc-rich multifunctional coatings, are emerging; these have the advantages of improving the anticorrosion properties by enhancing the physical barrier mechanism and cathodic protective effect.[10,11] The addition of nanostructures such as CNTs enhances both protective effects, thus allowing for better interconnectivity of Zn active particles by improving the electronic conduction of the epoxy matrix, owing to the high aspect ratio; these nanostructures also achieve a lower percolation threshold than other conductive particles, as described by Cubides et al.,[10,11] in zinc-rich epoxy primers containing multiwalled CNTs, with differing zinc content and fixed composition of CNTs. In the same context, Park and Shon[12] have demonstrated that increasing the content of multiwalled CNTs in epoxy coatings with different ratios of zinc dust results in higher conductivity, thereby improving the cathodic protection of carbon steel. Impedance measurements have confirmed the effects on corrosion protection.

Some researchers have evaluated Zn-rich epoxy primers in media containing sulfate-reducing bacteria.[6,13,14] In addition, previous work by Castaneda and Galicia,[15] in a comprehensive experimental platform, has characterized the electrochemical response of a dual-protection zinc epoxy coating with different ratios of additive CNTs to active zinc particles after exposure to a sulfate-reducing consortium. For zinc-rich epoxy (Zn-REP) coatings, despite the microbial-inhibiting effect of zinc surfaces, microorganisms in biofilms remain tolerant of many toxic materials that are effective against planktonic cells. As described by Ogawa et al.,[16] biofilm formation plays a crucial role in carbon steel corrosion, such that microorganisms can still damage the coating. Ding et al.[17] have revealed the high diversity of biofilm-forming microorganisms that can attach to zinc surfaces and adapt to toxic metal surfaces, thus highlighting the ability of microorganisms to attach to the surfaces of coatings and form biofilms. Biofilm structure provides substantial protection for bacterial cells and renders them highly resistant to detachment by physical forces and harmful nanoparticles.[18] The ostensible lethal effects of CNTs on biofilm formation have been studied to evaluate their potential to impede microorganism attachment and/or proliferation at different stages of bacterial colonization.[19]

Moreover, an approach to protect steel against corrosion via the formation of a biofilm of marine bacteria has recently been proposed in conjunction with the formation of an organic–inorganic hybrid film. This method has been successfully demonstrated in seawater with the marine bacterium *Pseudoalteromonas lipolytica*.[20] Previous work on protective biofilm formation in marine media on zinc-rich epoxy coatings has revealed a synergistic effect of biofilm formation in promoting a cathodic protective mechanism for Zn-REP with differing CNT content.[21] In a different approach, this study investigated the influence of different amounts of CNTs on the anticorrosive behavior of Zn-REP nanohybrids exposed to biofilm formation by a marine *Shewanella sp*. strain. These Gram-negative bacteria are rod-like and exist mainly in marine environments; they have a notable role in carbon steel corrosion. The main contribution of this study is monitoring the anticorrosion performance of Zn-REP coatings and the specific influence of *Shewanella sp*. over time through testing two different contents of CNTs. In addition, this investigation emphasized the specific role of biofilm formation, with an aim to elucidate the mechanistic anticorrosion aspects for each Zn-REP coating. Microorganism adherence to the coating was assessed, and the electrochemical activity was monitored with open-circuit potential (OCP) and electrochemical impedance spectroscopy (EIS). Surface analysis by scanning electronic microscopy (SEM) coupled to energy-dispersive X-ray spectroscopy (EDS) analysis was used to correlate the electrochemical behavior of hybrid zinc-rich epoxy-coated samples during 28 days at various intermediate exposure times.

2 | EXPERIMENTAL

2.1 | Marine bacterial strain culture preparation and incubation

Shewanella sp. was isolated from marine sediments obtained at 400-m depth from the Southern Gulf of Mexico near the Dos Bocas, Tabasco region. Bacteria were precultured at 37°C in 10 ml of Luria–Bertani (LB) nutrient broth, consisting of five yeast extract, 10 g tryptone, and 8 g NaCl (0.8% NaCl) in 1 L deionized water for 24 h.[21] Experimental cultures of each electrochemical cell were adjusted to 0.1 $OD_{600\,nm}$ in 25 ml of LB medium from preculture and were incubated inside the electrochemical cell in the presence of substrate/coating electrodes at 23°C.

2.2 | Experimental setup

Experiments were performed with a conventional 50 ml three-electrode glass cell. The coating/substrate samples consisted of UNS1008 carbon steel coated with Zn-REP nanohybrid coatings with dimensions of 10 × 11 mm; the

working electrodes were inserted in an epoxy resin. Three different coatings were used: Zinc epoxy primer (ZnR), zinc epoxy primer with CNTs (Zn-1×CNT), and zinc epoxy primer with twice the content of the prior formulation (Zn-2×CNT). The reference electrode was a saturated calomel electrode, and a platinum screen was used as a counter electrode. The external and internal surfaces of the glass cells were autoclaved. The working electrodes, the reference, and the auxiliary electrode were sterilized with 70% ethanol and acetone and set under UV light and laminar flow. The electrochemical setup included a VSP-300 potentiostat/galvanostat (Bio-Logic Science Instruments) with EC-Lab® V.10.32 software. The global experimental setup consisted of three electrochemical cells corresponding to each coating tested with inoculation of the *Shewanella sp*. strain and, as a control, another three electrochemical cells containing electrolyte without the bacterial strain.

2.3 | Electrochemical measurements

The electrochemical testing procedure consisted of the measurement of OCP and EIS for 28 days. OCP was measured 10 min before EIS measurements. EIS was performed at the OCP in a frequency range from 100 kHz to 10 MHz with 10 mV amplitude. All electrochemical experiments were performed in duplicate to ensure reproducibility. All tests were performed at 23°C.

2.4 | SEM sample preparation

ZnR, Zn-1×CNT, and Zn-2×CNT coated samples with biofilm coverage were washed twice with 1 ml of phosphate-buffered saline (PBS) (1×) and fixed with 2.5% glutaraldehyde in PBS for 24 h at 4°C. The samples were then washed with 1 ml of PBS (1×) three more times, followed by deionized water three times, for each treatment. The samples were dehydrated in an ethanol distilled water series of 50%, 75%, 95%, and 100% ethanol, for 10 min per dilution.[21] Samples were stored in airtight sealed glass. Immediately after the drying process, they were coated with gold/palladium particles and examined with a JEOL JSM-7000F SEM.

3 | RESULTS AND DISCUSSION

3.1 | OCP measurements

Figure 1 shows the OCP values of the coatings in sterile LB (control) and in the presence of *Shewanella sp*.

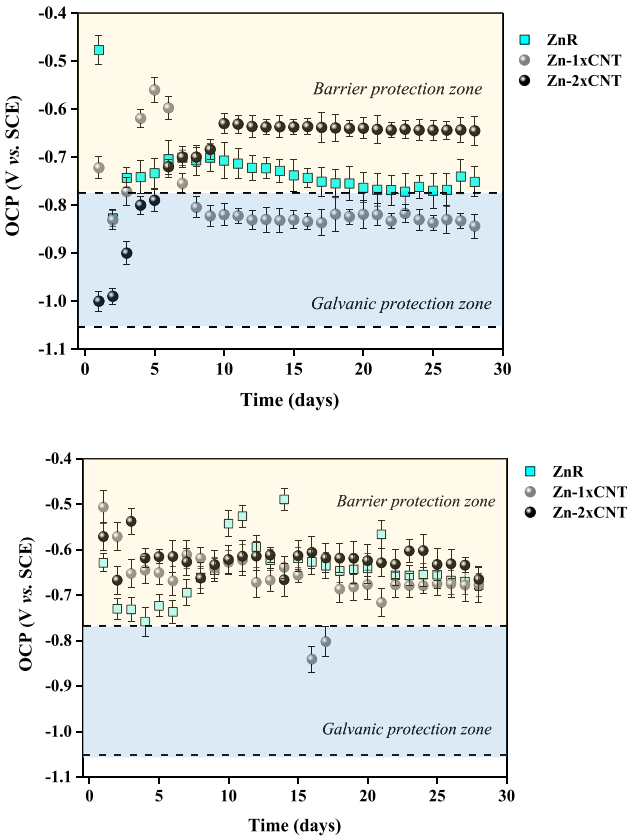

FIGURE 1 Open-circuit potential (OCP) measurements for each coating immersed in (a) Luria–Bertani control medium and (b) in the presence of *Shewanella sp*. strain. CNT, carbon nanotube; Zn-1×CNT, zinc epoxy primer with CNTs; Zn-2×CNT, zinc epoxy primer with twice the quantity of CNTs; ZnR, zinc epoxy primer [Color figure can be viewed at wileyonlinelibrary.com]

strain over the course of 28 days of exposure. The electrolyte effects in both abiotic and biotic medium promoted activation of the zinc particles at different exposure times, mostly under abiotic conditions. Under abiotic conditions, as presented in Figure 1a, the Zn-1×CNT and Zn-2×CNT coatings showed high potential variation in the first 5 days in which the potential shifted to more cathodic values (between −0.8 and −1 V vs. ECS); in accordance with the established criteria of protective potential, the E_{prot} value close to −0.774 V versus the saturated calomel electrode, as is generally accepted for carbon and low-alloy steels.[22] In an efficient cathodic protection system, the E_{prot} is in the range of −0.80 to −1.05 V versus ECS.[23] However, between Days 5 and 7, the potential became more continuous and stabilized after Day 10, when the Zn-1×CNT and Zn-2×CNT coatings showed a more uniform behavior, which remained within the galvanic protection zone for Zn-1×CNT and the barrier protection zone for Zn-2×CNT. OCP for zinc-rich epoxy coating maintained at the border

of the barrier protection zone/cathodic protection zone, a result mainly ascribable to the limited electrical contact between the zinc particles and the metallic substrate.

The OCP behavior of Zn-REP coatings in the presence of *Shewanella sp*. is shown in Figure 1b. All three Zn-REP coatings did not provide galvanic protection to the metallic substrate. This finding might indicate that a biofilm had formed at the surface of the coating since the beginning of the experiment. The presence of an external layer of semipermeable biomolecules, as exopolymeric substances, retards or delays the passage of ions and corrosive species present in bioelectrolytes. For the Zn-1×CNT, the potentials moved toward the cathodic protection region, with marked effects at Days 16 and 17. The change in the protective mechanism of the Zn-1×CNT coating may be attributed to the presence of CNTs because they notably increase the contact surface for a greater quantity of zinc particles and also improve the interconnectivity between Zn and CNTs additives, thus contributing to catalysis of the anodic reaction. The quantity of CNTs was sufficient to partially disrupt biological mechanisms in bacterial cells that impede bacterial attachment and formation of exopolymeric substances on the coating surface.[18]

The electrolyte uptake in the coatings activates the surfaces of the zinc particles, thus favoring the cathodic protective reaction and decreasing the useful life of the coating. Because of the greater quantity of zinc particles, the formation of zinc corrosion products such as $Zn(OH)_2$ and $ZnCO_3$ is possible, and these products remain embedded in the deposits of the epoxy coating, thus preventing the passage of external molecules toward the steel.[11] In the presence of *Shewanella sp*. this behavior shifted over time, and corrosion products were established on the surface of the coating.

The protective mechanism of the Zn-2×CNT coating was predominantly a barrier-protective mechanism, presumably because the concentration of CNTs does not affect bacterial attachment, and the amount of CNT used may promote the formation of a mature biofilm.[19]

OCP variations provided insight into the activity of the biofilm because the coverage was not continuous over long periods of time. On some days, the potential value was more cathodic, owing to the formation of a thicker biofilm, probably because the presence of a saturated distribution of CNTs influenced the formation of an exopolysaccharide (EPS) matrix through the interaction of the electrolyte with the conductive CNTs. This possibility is supported by observations by Bose et al.,[24] in which CNT-modified electrodes were found to be superior to planar electrodes for mixed consortium biofilm formation. This improvement was attributed to more favorable microbial adhesion provided by the CNT structure and not simply to the increased surface area.[25] Therefore, some cathodic potentials promote the formation of more homogeneous and dense biofilms in corrosive environments.

3.2 | Electrochemical impedance spectroscopy

3.2.1 | Uncoated UNS1008 steel

Through EIS, we monitored the electrochemical behavior of uncoated UNS1008 steel in LB medium under different conditions. A typical charge transfer process was observed in the absence of bacteria: The impedance plots showed a circular loop (Figure 2a) indicative of the anodic oxidation reaction of steel ($Fe^0 \rightarrow Fe^{2+} + 2e^-$). The maximum phase angle values ranged between −68° and −53° at low-intermediate frequencies (Figure 2b), thus suggesting that the capacitive response decreases over time primarily because of the rapid transformation of Fe^{2+} ions to corrosion products; therefore, when the corrosion progresses, the steel surface becomes less homogeneous, thus creating more reactive sites and favoring the degradation of the alloy.[26] When the *Shewanella sp*. strain was present in the LB medium, the impedance response (Figure 2c) was highly variable: The resistance values increased from Day 1 to Day 7, then decreased until Day 21, and apparently, no chemical process other than that described above was observed. However, the Bode plot (Figure 2d) showed a second time constant that appeared on Day 21 and was more evident by Day 28; this phenomenon is attributable to the formation of bacterial biofilm, as described by Castaneda and Galicia.[15]

The equivalent circuits (EC) used to describe the above systems are shown in Figure 3. In the absence of *Shewanella sp*. strain, the circuit detailed in Figure 3a (one electrochemical reaction) was used. In the presence of the bacteria in LB medium, the EC shown in Figure 3b was chosen, taking into account the second time constant, where R_{ct} is the charge transfer resistance of the steel alloy, and $R_{ct\text{-}b}$ is the resistance of the biofilm. The capacitance of the electrochemical interface and biofilm was represented with a constant phase element (CPE) to approximate the nonideal behavior of the capacitor due to surface defects.[27] The CPE impedance (Z_{CPE}) describes the dielectric properties of the electrochemical interface according to the following equation:

$$Z_{CPE} = \frac{1}{Y_0(j\omega)^n}, \quad (1)$$

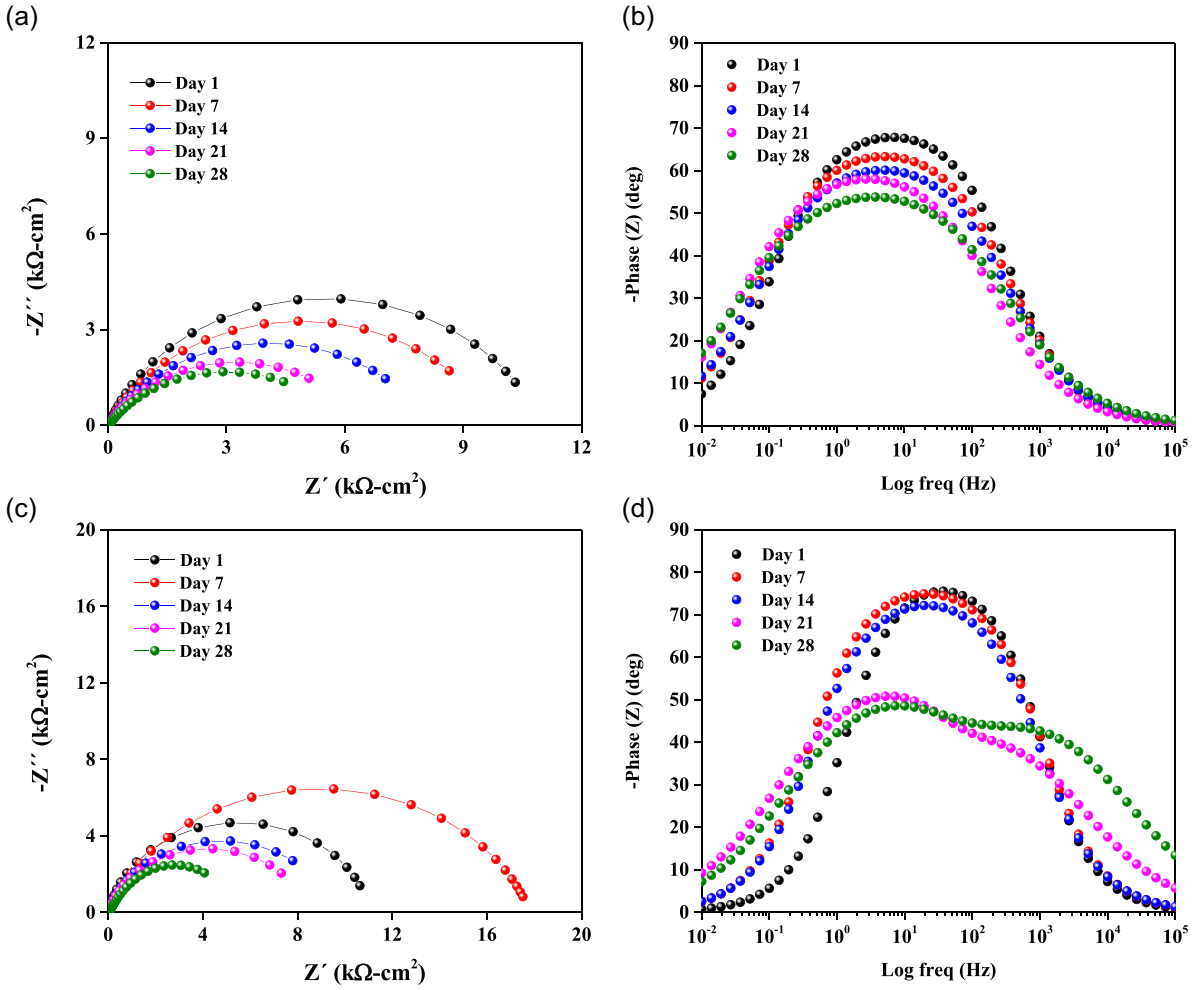

FIGURE 2 Nyquist and Bode plots of uncoated UNS1008 steel, during 1–28 days of exposure in the absence (a,b) and presence (c,d) of *Shewanella sp.* strain in Luria–Bertani medium [Color figure can be viewed at wileyonlinelibrary.com]

where ω is the angular frequency, with $\omega = 2\pi f$ (and f being the frequency), "j" is $\sqrt{-1}$, and Y_0 is a constant parameter with units of $s^n\,\Omega^{-1}$ related to "n," which measures the deviation from ideal behavior as well as the effect of the repulsion or accumulation of electric charges when a specific value is used; for an ideal capacitor, $n = 1$ represents a pure capacitance line.[28] Therefore, the capacitance (C) was calculated from the CPE parameter Y_0 by using the following equation:

$$C = Y_0(\omega''_m)^{n-1}, \tag{2}$$

where ω''_m is the maximum angular frequency in the Nyquist plot on the y-axis (imaginary impedance) with the highest value of Z_{imag}.[29]

As shown in Table 1, in the absence of the bacteria, the values of R_{ct} progressively decreased from 10,942 to 5986 $\Omega\,cm^2$ over the 28 days of monitoring. This behavior was expected because of the exposure of steel alloy to a corrosive medium, and mainly the presence of Cl^- ions in the aerobic medium, in which the hydronium ion cathodic reduction ($2H^+ + 2e^- \rightarrow H_2$) completes the redox pair, thus favoring corrosion of the alloy. In the presence of the *Shewanella sp.* strain, the first 14 days showed variable behavior with an increase in R_{ct} in the transition from Days 1 (11,026 $\Omega\,cm^2$) to 7 (17,812 $\Omega\,cm^2$) and a subsequent decrease on Day 14. These variations in resistance have been linked to the initial stage of biofilm formation when an EPS matrix is consolidated along the metal surface; this matrix has been reported to have a protective effect against corrosion.[30,31] Subsequently, a significant decrease was observed in the R_{ct} on Day 28, with a value of 5229 $\Omega\,cm^2$. These results are attributable to the maturation of the biofilm and imply that the microbial influence on corrosion, in this case by the *Shewanella sp.* strain, is favorable under these conditions through an extracellular electronic transfer mechanism of microbially influenced corrosion (EET-MIC). As reported by Kalnaowakul et al.,[32] in this mechanism, the bacteria use the iron directly as an electron donor.

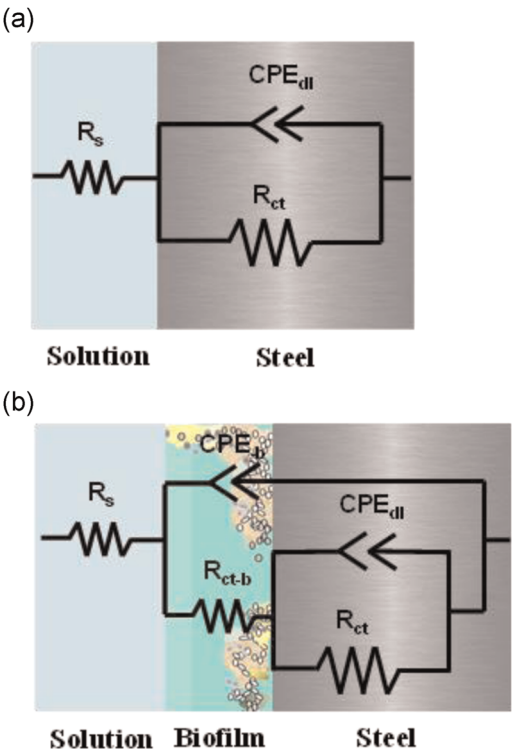

FIGURE 3 Equivalent circuits used for modeling the electrochemical impedance spectroscopy results of uncoated UNS1008 steel from 1 to 28 days of exposure [Color figure can be viewed at wileyonlinelibrary.com]

Biofilm formation acts as a barrier that does not allow the byproducts of bacterial metabolism to diffuse from the interphase to bioelectrolyte. This aspect explains the large accumulation of charges at the interface ($CPE_1 = 646.3$ $s^n\,\Omega^{-1}\,cm^{-2}$ at Day 28); it is also important to consider that a heterogeneous biofilm had formed, given the values of n_2 of 0.64 and 0.72, which were far from the ideal value. The iron oxidized through an EET-MIC mechanism begins a localized corrosion process and, by pitting, subsequently generally damages the integrity of the alloy.[33]

3.2.2 | ZnR coating

The Nyquist plot of the ZnR coating (Figure 4a) showed an undefined loop with impedance values much higher than those of uncoated steel during the first 14 days. After Days 21 and 28, diffusion of ionic species, corrosion products, and organic molecules predominated in the interfacial reactions because the slope was close to 45° at low frequencies.[34] In the Bode plot (Figure 4b), two time constants were observed at low-intermediate frequencies on Day 1. These results describe the activation of the zinc particles and the formation of a mixed layer on the interface, composed of the epoxy coating and accumulated organic matter (carbohydrates and proteins), as observed in the uncoated steel on Days 21 and 28. The time constant observed at low frequencies represented the anodic oxidation reaction of zinc ($Zn^0 \rightarrow Zn^{2+} + 2e^-$). This reaction is not expected to predominate in this system because, as observed in the OCP in the absence and presence of the bacteria, the coating provided a barrier-protective mechanism throughout the 28 days of monitoring, possibly because of the poor interconnection of the zinc particles inside the epoxy might have resulted in

TABLE 1 Fitting parameters of equivalent circuit simulation of uncoated UNS1008 steel during the 28 days in the absence and presence of *Shewanella sp.* strain

Time (day)	R_s (Ω cm^2)	CPE_{dl} ($s^n/\ \Omega$ cm^2)	n_1	R_{ct} (Ω cm^2)	CPE_b ($s^n/\ \Omega$ cm^2)	$R_{ct\text{-}b}$ (Ω cm^2)	n_2	χ^2
−*Shewanella sp.*								
1	16.5	125.3	0.8	10,942	-	-	-	3.4×10^{-4}
7	15.9	191.2	0.7	9765	-	-	-	2.7×10^{-4}
14	17.4	236.6	0.7	8106	-	-	-	3.1×10^{-4}
21	16.1	412.6	0.7	6452	-	-	-	5.6×10^{-4}
28	14.7	453.4	0.7	5986	-	-	-	4.2×10^{-4}
+*Shewanella sp.*								
1	14.4	149.7	0.8	11,026	-	-	-	0.9×10^{-3}
7	15.8	26.4	0.8	17,812	-	-	-	5.5×10^{-4}
14	16.5	33.1	0.9	9514	-	-	-	9.8×10^{-4}
21	20.7	121.5	0.7	8452	21.7	543	0.6	1.2×10^{-3}
28	26.3	646.3	0.7	5229	23.4	756	0.7	4.7×10^{-3}

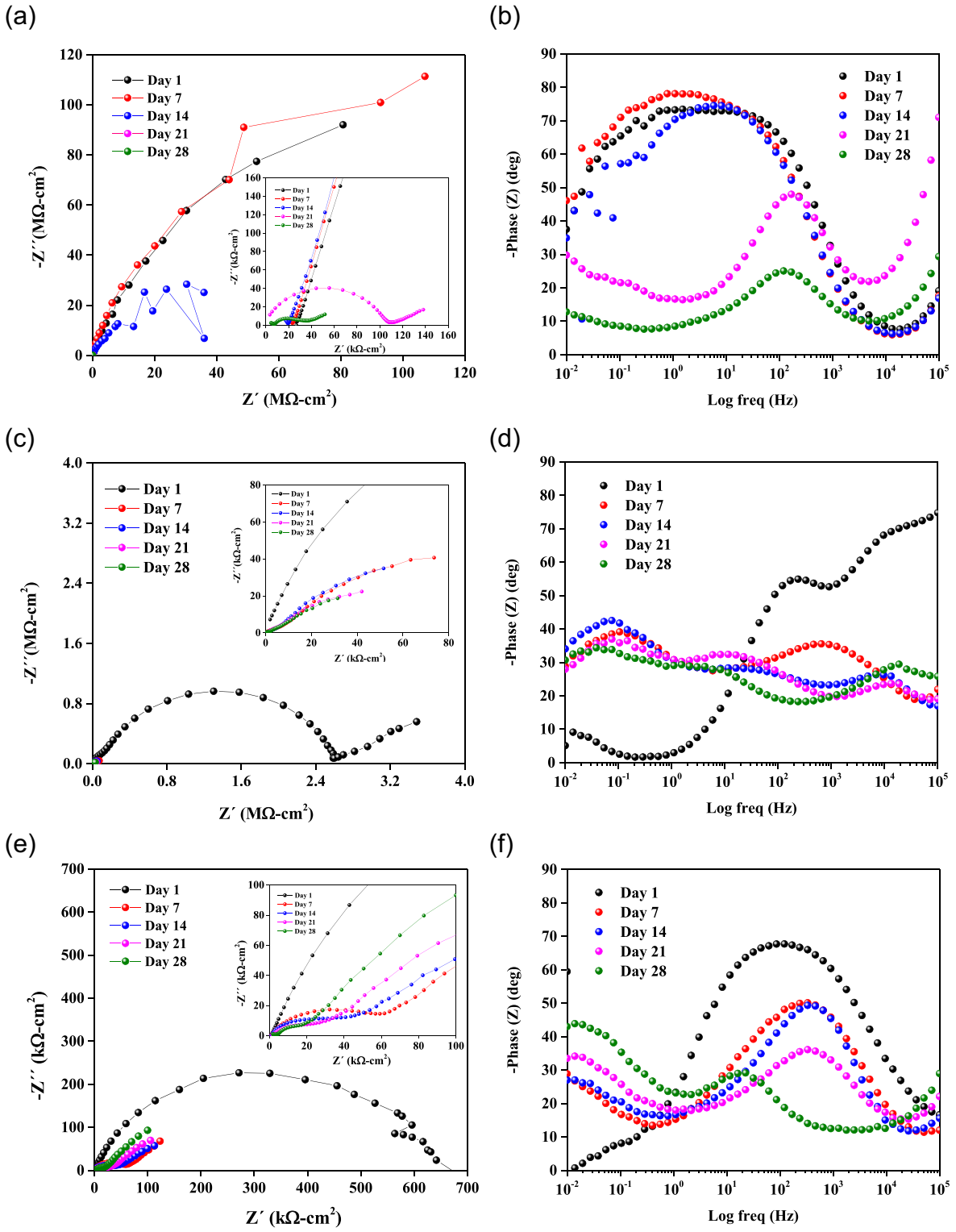

FIGURE 4 Nyquist and Bode plots obtained during 28 days in Luria–Bertani medium with *Shewanella sp.* strain exposed to coatings: (a, b) Zinc epoxy primer, (c,d) zinc epoxy primer with CNTs, and (e,f) zinc epoxy primer with twice the quantity of CNTs. CNT, carbon nanotube [Color figure can be viewed at wileyonlinelibrary.com]

a small contact area for the galvanic reaction.[35] On Days 21 and 28, a time constant was observed at intermediate frequencies with maximum phase angles of −48° and −25°, respectively. The results revealed an increase in the resistance of the solution, thus indicating the exhaustion of most zinc particles, owing to conversion to insoluble corrosion products, such as ZnO and $Zn(OH)_2$, which occupied the reactive sites where the particles were found.

Consequently, the transport of corrosive ions and the contact of bacteria on the surface of the alloy were partially hindered, and the impedance response continued to decrease. Furthermore, the results indicated the formation of a slightly compact mature biofilm composed of a heterogeneous layer of EPS, products of corrosion, and precipitates, as described by Castaneda and Galicia,[15] which showed a significant effect on corrosion from Day 21.

3.2.3 | Zn-1×CNT coating

The results of the Zn-1×CNT coating in the biotic medium are shown in Figure 4c,d. The addition of a CNT equivalent had an important effect because a more complex system was observed than that with the ZnR coating. On Day 1, a diffusion-controlled charge transfer process was recorded with a high impedance value, which then substantially decreased. In the subsequent days, a second loop appeared, which indicated the rapid dissolution of the zinc particles according to OCP observations that indicated a galvanic protective mechanism from Day 8 in the absence of the *Shewanella sp*. strain. These results are attributable to an improvement in the electrical properties of the coating due to the presence of CNTs, which also provided a greater surface area,[36] forming more reactive sites, favoring charge transfer at the biofilm/coating interface. In contrast, after Day 14, a third time constant appeared, which indicated the formation of a mature biofilm. This process was in constant competition with the oxidation of steel and the galvanic reaction; however, the experimental data showed that the effect of the biofilm prevailed because in the Zn-1×CNT coating, in contrast to the ZnR coating, most of the zinc particles dissolved before the consolidation of the biofilm and the diffusion of the corrosion products into the solution. Therefore, the contact of bacteria on the alloy was not hindered by contributing to the anodic oxidation of the alloy through the EET-MIC mechanism.

3.2.4 | Zn-2×CNT coating

The results of the Zn-2×CNT coating are shown in Figure 4. According to the Nyquist plot (Figure 4e), from Day 7 to Day 28, a loop in the impedance diagram was observed, indicating a controlled charge transfer process by diffusion. The addition of two equivalents of CNTs improved the coating's protective properties, as seen in the phase angle signature (Figure 4f), because only one time constant was observed. The data suggested that the activation and dissolution of the zinc particles occurred progressively during the initial stage of biofilm formation, which did not allow adhesion and significantly limited the contact of the *Shewanella sp*. strain with the steel surface. This idea is attributed to the existence of a greater contact area for the zinc particles and the improvement in electronic interconnectivity by the CNTs. Therefore, the formation of more zinc products is important because it does not allow the formation of a homogeneous biofilm, as seen in the impedance spectrum, in which the formation/initiation of an EPS matrix was observed. Furthermore, several studies have shown the inhibitory effects of zinc products,[37,38] mainly ZnO, which is toxic to some cellular elements in bacteria.[39] Therefore, no significant effects of the biofilm were observed in the corrosion process of the alloy, although the zinc particles had not dissolved. The results obtained were consistent with the OCP because, in the presence of the strain, a barrier-protective mechanism was seen throughout the monitoring. However, the zinc particles did not oxidize quickly, owing to the galvanic effect, thus hindering the contact of the bacteria through the progressive formation of ZnO and $Zn(OH)_2$. Therefore, the coating/biofilm was composed of zinc corrosion products

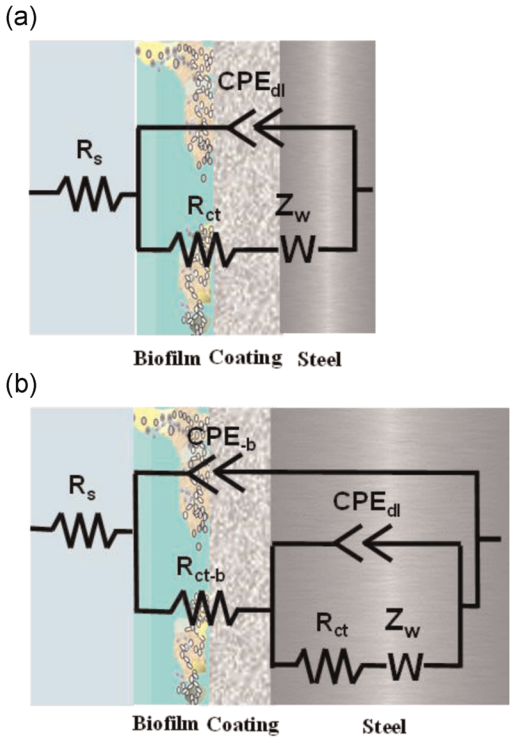

FIGURE 5 Equivalent circuits used for modeling the electrochemical impedance spectroscopy results of coated UNS1008 steel from 1 to 28 days of exposure in the presence of *Shewanella sp.* [Color figure can be viewed at wileyonlinelibrary.com]

TABLE 2 Fitting parameters of equivalent circuit simulation of coated UNS1008 steel during the 28 days in the presence of *Shewanella sp.* strain

Time (day)	R_s (Ω cm^2)	CPE_{dl} (s^n/ Ω cm^2)	W_{diff} (Ω cm^2)	R_{ct} (Ω cm^2)	CPE_b (s^n/ Ω cm^2)	$R_{ct\text{-}b}$ (Ω cm^2)	n	χ^2
Zn								
1	3731	33.7×10^{-3}	8721	2.37×10^{8}	27.1×10^{-6}	23,267	0.9	1.6×10^{-4}
7	2332	49.8×10^{-3}	20,565	2.87×10^{8}	-	-	-	2.5×10^{-3}
14	1973	67.9×10^{-3}	43,276	34.5×10^{6}	-	-	-	3.1×10^{-1}
21	1783	1.7×10^{-3}	6632	111,863	-	-	-	3.9×10^{-4}
28	630	1.66	3725	30,469	-	-	-	4.7×10^{-4}
Zn-1×CNT								
1	280	2.51×10^{-3}	165,750	2.19×10^{6}	3.53×10^{-3}	379,091	0.9	3.6×10^{-3}
7	258	3.08	21,593	5865	7.97	865	0.5	9.2×10^{-4}
14	119	111	5900	334.5	62.91	36,467	0.4	6.7×10^{-4}
21	79	315	38,045	946.8	43.57	2843	0.6	1.2×10^{-3}
28	61	637	37,549	579.3	1.61	949	0.4	2.7×10^{-4}
Zn-2×CNT								
1	937	6.02	8630	625,450	-	-	-	5.7×10^{-3}
7	1206	0.92	17,030	55,107	-	-	-	1.2×10^{-4}
14	1349	0.88	17,579	37,740	-	-	-	7.3×10^{-4}
21	1466	2.65	18,964	28,443	-	-	-	4.5×10^{-3}
28	1933	14.2	44,982	22,022	-	-	-	4.3×10^{-3}

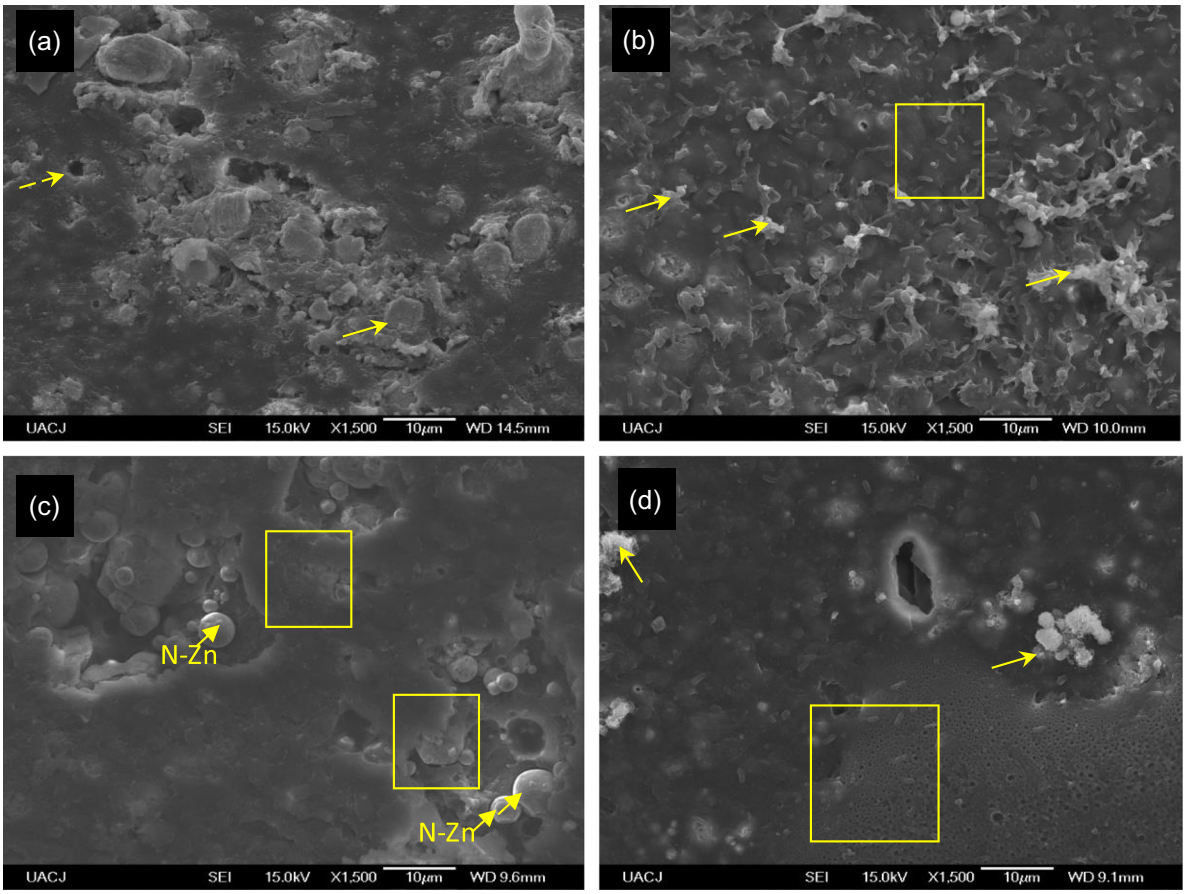

FIGURE 6 Scanning electron microscopy images of biofilms formed by *Shewanella sp.* strain in the presence of the zinc-rich epoxy primer. The strain adhesion was monitored after immersion in Luria–Bertani medium: (a) 7 days, (b) 14 days, (c) 21 days, and (d) 28 days [Color figure can be viewed at wileyonlinelibrary.com]

and biomolecules (EPS and proteins), which gradually diffused into the solution, thus increasing the resistance of the medium. Therefore, the phase angle decreased from −68° to −29° at the transition from Day 1 to Day 28, respectively, as observed in the ZnR coating.

The impedance parameters were obtained after fitting the EIS experimental results with the EC displayed in Figure 5, in the steel-coating-biofilm system in which $R_{ct\text{-}b}$ and CPE_b correspond to the pair coating-biofilm, and R_{ct} and CPE_{dl} correspond to steel. To describe the effect of diffusion, we added Warburg impedance to the circuit.[40]

The simulation results are shown in Table 2, which were adjusted to the circuits used because the values of χ^2 were in the range of 10^{-3} and 10^{-4}. For the ZnR coating, the R_{ct} decreased over time, from $2.87 \times 10^8\ \Omega\ cm^2$ on Day 7 to 30,469 Ω cm^2 on Day 28. This lower resistance magnitude was consistent with the results observed at the OCP for this coating, thus indicating a loss of biofilm formation as the surface became more active, which subsequently diminished the barrier effect and greatly influenced the charge transfer of the system. The same behavior was observed for the Zn-2×CNT coating: The R_{ct} decreased from 625,450 Ω cm^2 on Day 7 to 22,022 Ω cm^2 on Day 28. The magnitudes for this coating were minor in proportion to the ZnR coating, a result attributable to charge transfer processes preferentially occurring because of the interconnectivity between CNTs and Zn particles. ZnR particles are distributed and react with electrolytes, thus forming Zn corrosion products, as previously characterized by Cubides et al.[11] Both the ZnR and Zn-2×CNT coatings showed lower R_{ct} values than uncoated steel on Day 28. This result demonstrated the effectiveness of the coatings under biotic conditions. In the case of the Zn-1×CNT coating, the low R_{ct} values represented a favorable galvanic reaction in the corrosive medium, indicating the rapid dissolution of the zinc particles through their wetting and activation. The values of n (0.4–0.5) indicated an inhomogeneous biofilm, which might not have been consolidated throughout the surface; however, the biofilm resistance values ($R_{ct\text{-}b}$) were higher than those of the alloy. These results showed the effect of the scarce EPS synthesized by the bacterial strain, indicating unfavorable adhesion on the coating.

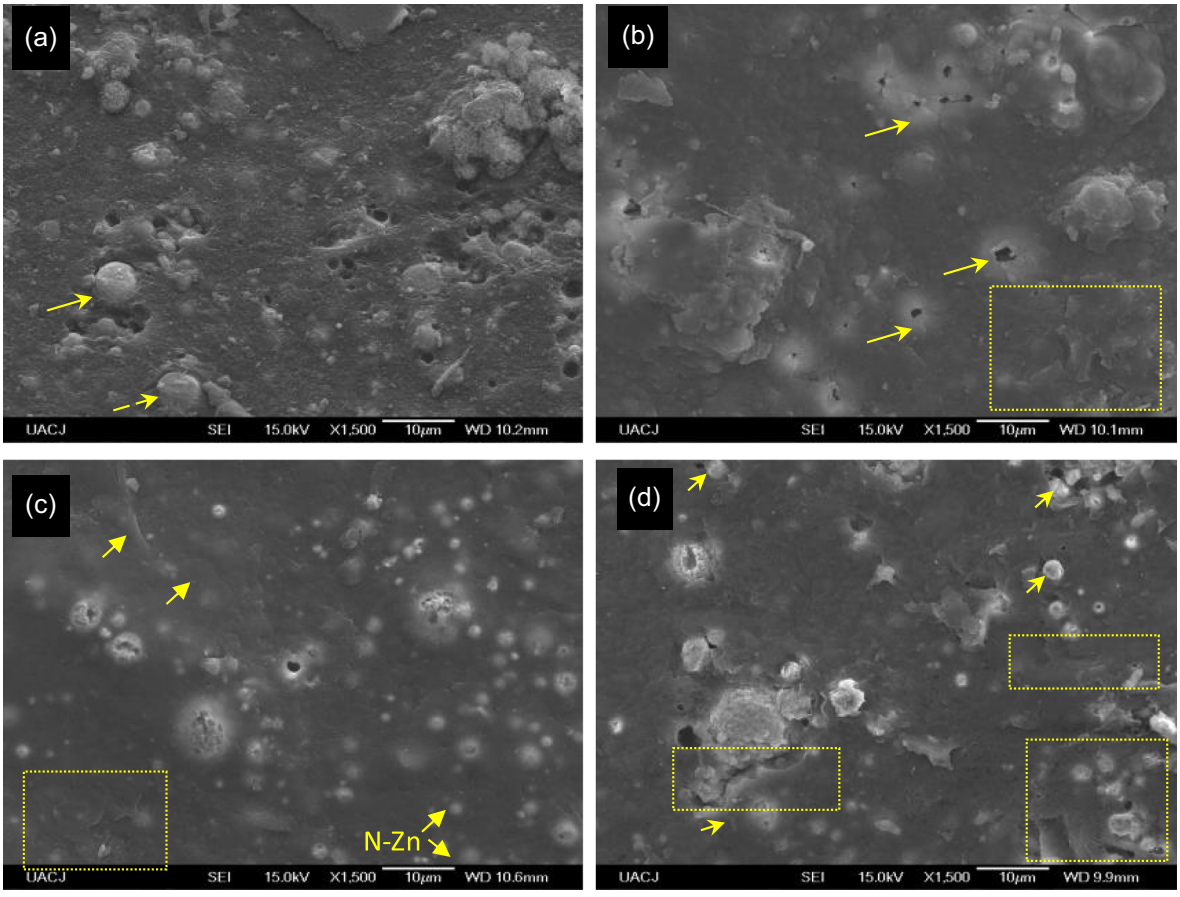

FIGURE 7 Scanning electron microscopy images of biofilm formed by *Shewanella sp.* strain onto Zn-1×CNT primer. The strain adhesion was monitored after immersion in Luria–Bertani medium: (a) 7 days, (b) 14 days, (c) 21 days, and (d) 28 days. Zn-1×CNT, zinc epoxy primer with CNTs [Color figure can be viewed at wileyonlinelibrary.com]

3.3 | Qualitative analysis by SEM-EDS

Figure 6 shows SEM images obtained for Zn-REP over the course of 28 days of immersion in the presence of the *Shewanella sp*. strain. As shown in Figure 6a, some amorphous components were associated with zinc corrosion products, as previously described by Cubides and Castaneda[11,12] for these nanohybrid coatings. The effects of corrosion products were previously observed during OCP monitoring at 7 days. Cellular ultrastructure and EPS were detected in SEM images in Figure 6b. The morphology of cells corresponded to planktonic, rod-shaped *Shewanella sp*. cells and dimensions of approximately 2–4- and 0.4–0.7-μm diameter. The cells began to appear more embedded in an exopolymeric matrix of microbial biofilm after Day 14 (Figure 6c,d). Figure 6b–d shows the formation of a layer of biofilm and a large number of sessile bacteria remaining at the Zn-coated surface. Because zinc oxide nanoparticles are antibacterial, they inhibit the growth of microorganisms by permeating the cell membrane.[40] Oxidative stress damages lipids, carbohydrates, proteins, and DNA.[41]

In the case of coating with Zn-1×CNT, the same structures of zinc corrosion products were present at 7 days (Figure 7a). Incipient formation of an exopolymeric matrix for microbial biofilm formation was evident on day 14, and planktonic cells of *Shewanella sp*. remained present (Figure 7b). The observation of a more compact and denser biofilm after Dasy 21 and 28, as evident in Figure 7c,d, was ascribed to the presence of CNTs in this type of coating. CNTs promote the formation of a denser biofilm after an active/mature biofilm forms on the surface, as previously reported by Upadhyayula and Gadhamshetty.[19] In this context, if the inherent cytotoxic nature of CNTs can be mitigated, CNTs may serve as substrates to immobilize selected biofilms. In this respect, the adherence of biofilm is promoted in the groove openings formed between CNT bundles and the outside surface area of CNT bundles because these regions are accessible to large sorbate species, such as bacteria.

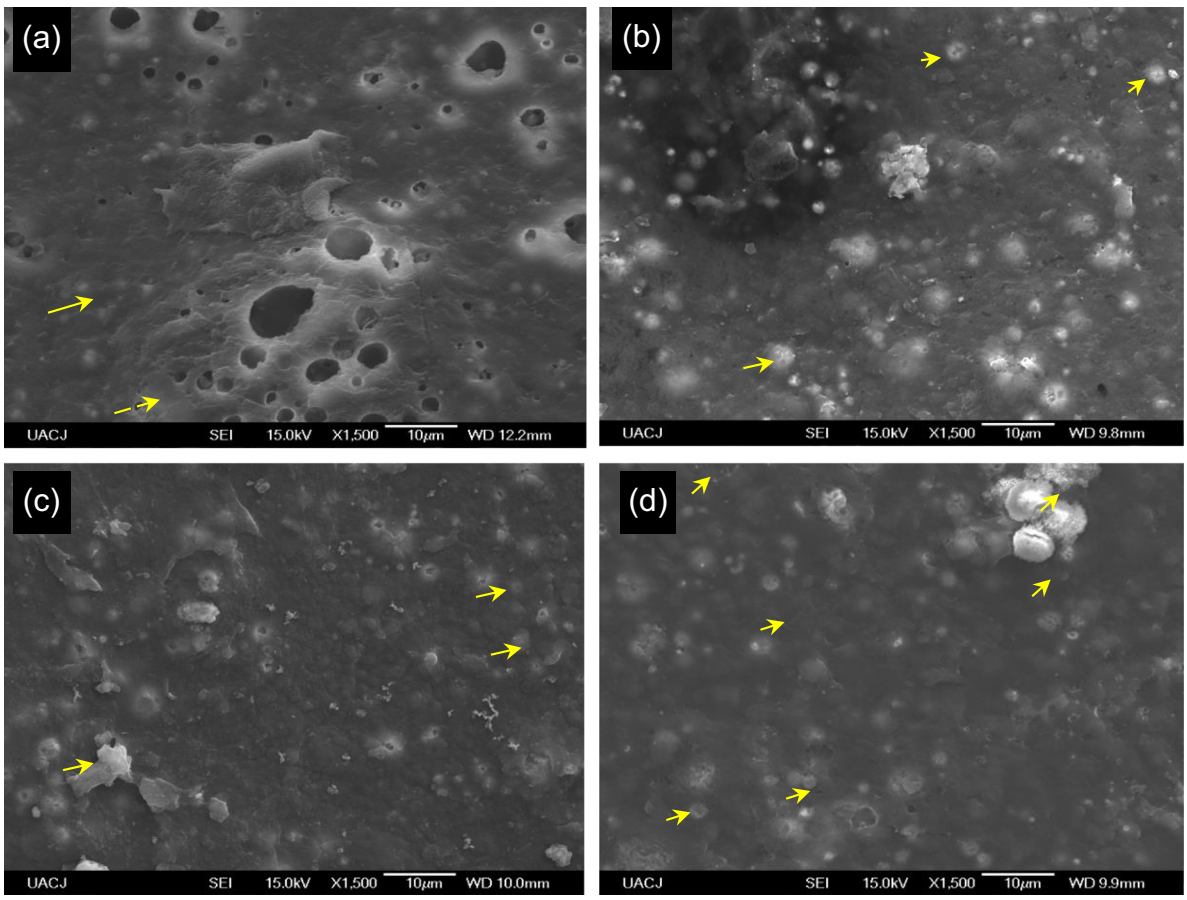

FIGURE 8 Scanning electron microscopy images of biofilm formed by *Shewanella sp*. strain onto Zn-2×CNT primer. The bacterial adhesion was monitoring at different immersion days in Luria–Bertani medium: (a) 7 days, (b) 14 days, (c) 21 days, and (d) 28 days. CNT, carbon nanotube; Zn-2×CNT, zinc-rich epoxy primer with twice the quantity of CNTs [Color figure can be viewed at wileyonlinelibrary.com]

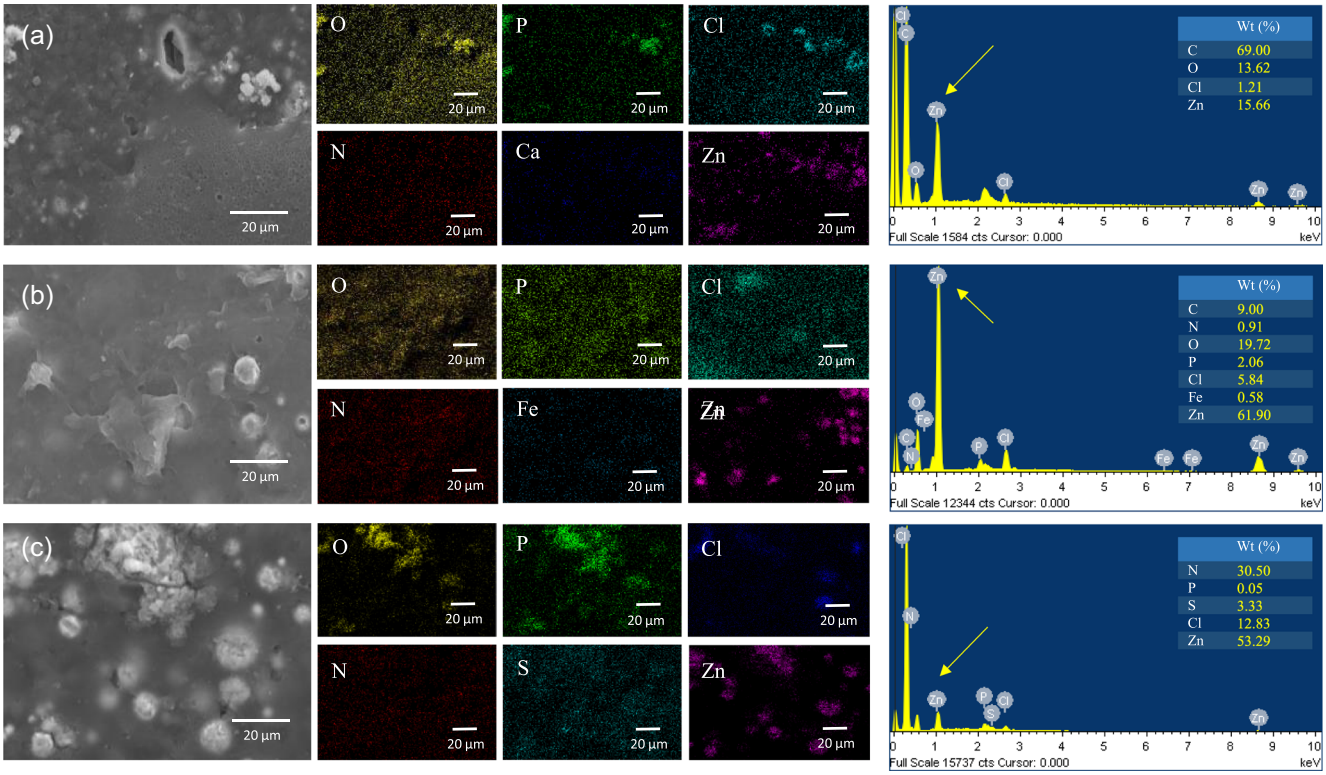

FIGURE 9 Cross-sectional SEM and EDS element mapping of coated UNS1008 steel after 28 days in the presence of *Shewanella sp*. strain in LB medium: (a) Zinc epoxy primer, (b) zinc epoxy primer with CNTs, and (c) zinc epoxy primer with twice the quantity of CNTs. CNT, carbon nanotube; EDS, energy-dispersive X-ray spectroscopy; SEM, scanning electron microscopy [Color figure can be viewed at wileyonlinelibrary.com]

Biofilm formation was promoted by the CNT adherence sites, as seen in our previous studies.[15,21] The content of zinc particles became less evident, as shown in Figure 7b,c, because they could not react with CNTs. Instead, the CNTs, rather than the interconnectivity between zinc particles, were more responsible for the biofilm formation. Figure 9 shows SEM images of biofilms formed by the *Shewanella sp*. strain on all coatings during 7 days of exposure in which the presence of bacteria, exopolymeric matrix and biofilm formation, and of phosphorous, chlorine, oxygen and sulfur, can be seen.

SEM images of the coating with twice the content of CNT, Zn-2×CNT, are shown in Figure 8, in which the lethal effects of CNT quantity on biofilm formation were evident for this coating. This adverse effect impeding microorganism attachment and proliferation at different stages of bacterial colonization was previously investigated.[21] Although the biofilm structure provides substantial protection for bacterial cells and renders them highly resistant to detachment by physical forces and harmful nanoparticles, CNTs had strong bactericidal activity toward cells in biofilms, as shown in Figure 8a,b. The initial biofilm formation disappeared, as shown in Figure 8c,d. In a previous study, a microscopic examination of the bottom layers of the biofilms of *Escherichia coli* and *Bacillus subtilis* in direct contact with coatings containing SWCNT revealed that ~80%–90% of the microbial cells were dead.[18] Moreover, the interaction of CNTs with biofilm is highly dependent on the stage of biofilm formation, and the efficacy of CNTs is more pronounced in the early stages of biofilm formation.[18] After microorganisms are protected within the structure of a mature biofilm, they are less susceptible to the influence of CNTs than bacteria in other biofilm phases.

In this respect, it is important to consider that the physicochemical properties of a surface, particularly composition, roughness, charge density, or hydrophobic/hydrophilic and lipophobic/lipophilic nature, are known to influence biofilm formation.[17]

The elemental composition of the 1008 carbon steel samples with coatings was analyzed after 28 days in bioelectrolyte by using EDS. The results obtained (Figure 9) allowed for the detection of oxygen, nitrogen, phosphorus, and sulfur in the three coatings, thus indicating the presence of macromolecules that indirectly indicated the formation of biofilms of *Shewanella sp*. on the coatings. According to Tong et al.,[42,43]

the distribution of oxygen and chlorine indicated the corrosion products of zinc, such as $ZnCl_2$ and ZnO, which, according to the images, were present in a smaller proportion in the coating of Zn-2×CNT, as shown and described in the EIS results. In contrast, the percentage composition by weight (wt%) indicated the effect of the CNTs because higher percentages of zinc were found in the coatings of Zn-1×CNT (61.9%) and Zn-2×CNT (53.29%). In addition, the results were consistent with the description of the OCP and the SEM images because

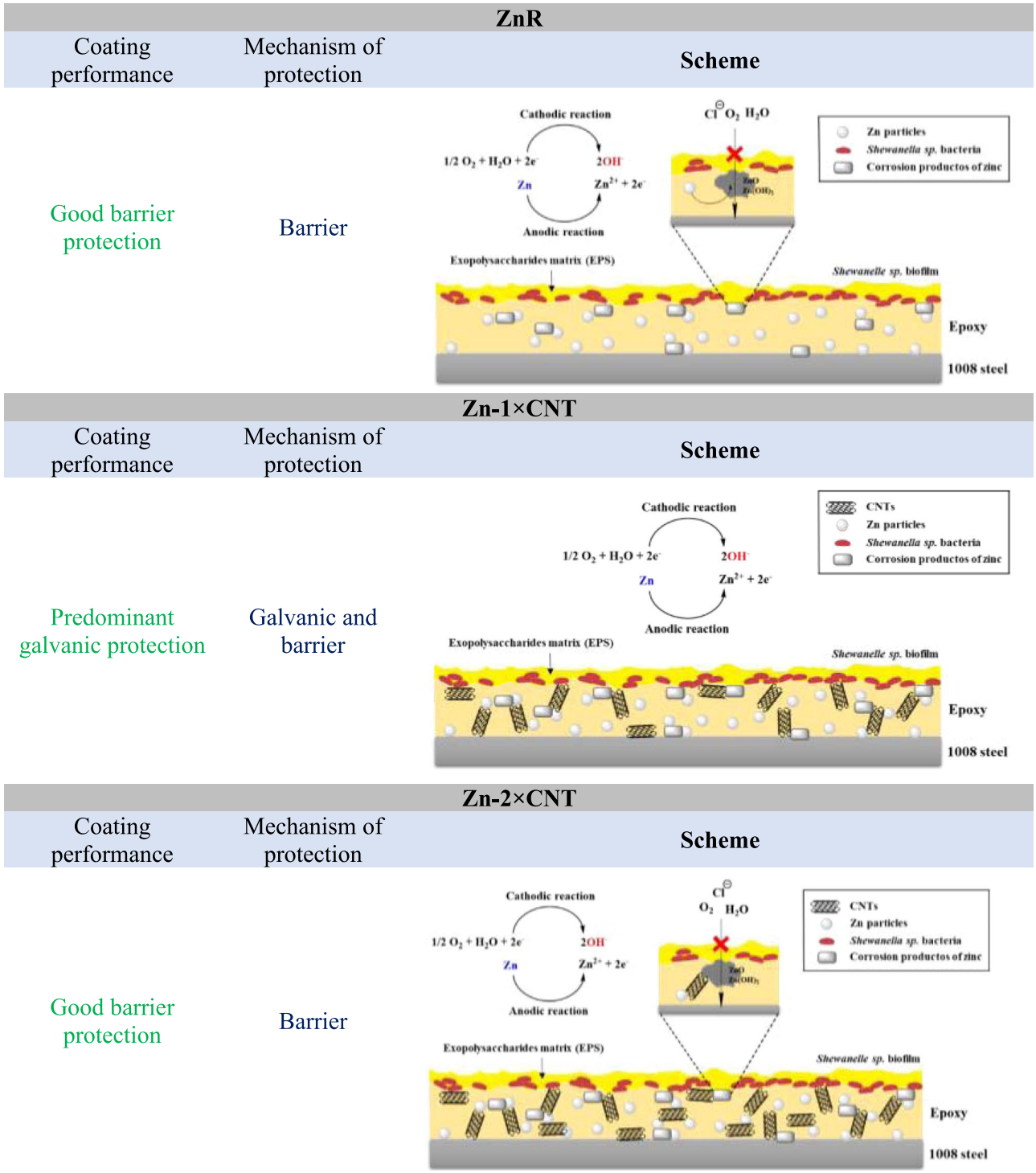

FIGURE 10 Behavior and protection mechanism of coatings applied to UNS1008 steel coated after 28 days in the presence of *Shewanella sp*. strain in Luria–Bertani medium. CNT, carbon nanotube; Zn-1×CNT, zinc epoxy primer with CNTs; Zn-2×CNT, zinc epoxy primer with twice the quantity of CNTs; ZnR, zinc epoxy primer [Color figure can be viewed at wileyonlinelibrary.com]

these coatings had a higher wt% of nitrogen, phosphorus, and oxygen, thus indicating the formation of a biofilm that was mostly consolidated and mature at the surface.

3.4 | Mechanism of corrosion protection in the presence of *Shewanella sp*.

According to the experimental results and the SEM images described above, the corrosion-protective mechanisms are proposed in Figure 10. As shown in Figure 10, the Zn-1×CNT coatings primarily had a cathodic protective mechanism, and the ZnR and Zn-2×CNT coatings exhibited a barrier-protective mechanism. The Zn-2×CNT was most efficient, owing to the evolution of a more cathodic OCP and less biofilm formation of *Shewanella sp*. on the surface. The impedance experiments revealed a marked difference between the galvanic and barrier-protective mechanisms, with the barrier protection yielding better results, as reflected in the lower R_{ct} on Day 28. According to Sorensen et al.,[44] the anodic oxidation of metallic zinc in a Fe–Zn-H_2O–Cl system indicates the precipitation of insoluble corrosion products that are more voluminous than ZnO and $Zn(OH)_2$, such as $ZnFe_2O_4$ near the sites of defects in the epoxy coating, thus further preventing the passage of oxidizing species toward the steel.[45]

4 | CONCLUSIONS

1. Favorable conditions for long-lasting settlement of biofilms were detected with Zn coatings during 28 days of immersion. This finding is explained by the interconnectivity between zinc particles providing a suitable surface for settlement and biofilm formation by *Shewanella sp*.
2. Addition of CNTs promoted biofilm formation after 14 days of *Shewanella sp*. strain exposure. Enhanced corrosion resistance of Zn-1×CNT epoxy was evident in the presence of marine bacteria.
3. However, using twice the content of CNTs in zinc-rich epoxy coatings unfavorably influenced the formation and distribution of biofilm at the surface of the coating, owing to a lethal effect.
4. OCP and EIS monitoring showed that marine biofilm settlement helps to produce a barrier effect rather than a cathodic protective effect, owing to mass transfer control.
5. Impedance diagrams revealed adherence and attachment of *Shewanella sp*. after biofilm formation starting from the first day of immersion in Zn-REP. However, an ulterior detachment was appreciated. Activation of zinc particles after the detachment of bacteria became evident.

ACKNOWLEDGMENTS

The authors thank Graciela Garcia for assistance in marine sediment management as well as Sandra Núñez for microbiological manipulation and Dra. Marisela Aguirre for valuable discussions and marine bacterial isolation, finally Ivan Salcido for technical assistance in obtaining SEM images.

CONFLICT OF INTERESTS

The authors declare that there are no conflict of interests.

DATA AVAILABILITY STATEMENT

Research data are not shared.

ORCID

Monica Galicia Garcia http://orcid.org/0000-0003-1273-3204

REFERENCES

[1] O. Medina, A. Ortiz, V. H. Jacobo, R. Schouwenaars, *Ing. Invest. Tecnol.* **2009**, *1*, 9.
[2] A. Kumar, L. Huan-Hsuan, P. Kavanangh, F. Barriere, L. Lapinsonniere, J. Lienhard, *Nat. Rev.* **2017**, *1*, 145.
[3] D. Inbakandan, C. Kumar, L. Stanley, R. Kirubagaran, R. Venkatesan, S. Ajmal, *Colloids Surf. B Biointerfaces* **2013**, *111*, 636.
[4] H. Castaneda, X. Benetton, *Corros. Sci.* **2008**, *50*, 1169.
[5] Y. Chen, Q. Tang, J. Senko, G. Cheng, B. Zhang, H. Castaneda, L. Ju, *Corros. Sci.* **2015**, *90*, 89.
[6] A. Abdolahi, E. Hamzah, Z. Ibrahim, S. Hashim, *Polym. Rev.* **2014**, *54*, 702.
[7] M. Fedel, F. Rodríguez, S. Rossi, F. Deflorian, *Coatings* **2019**, *9*, 680.
[8] C. M. Abreu, M. Izquierdo, P. Perino, X. Novoa, C. Pérez, *Corrosion* **1999**, *55*, 1173.
[9] S. Tambe, S. Jagtap, A. Chaurasiya, K. Joshi, *Prog. Org. Coat.* **2016**, *94*, 49.
[10] Y. Cubides, H. Castaneda, *Corros. Sci.* **2016**, *109*, 145.
[11] Y. Cubides, S. Su, H. Castaneda, *Corrosion* **2016**, *72*, 1397.
[12] S.-M. Park, M.-Y. Shon, *J. Ind. Eng. Chem.* **2015**, *21*, 1258.
[13] J. Wang, Q. Li, Y. Fu, C. Li, *Key Eng. Mater.* **2012**, *488*, 262.
[14] D. Liu, Q. Fe, C. Hui, L. Li, *Key Eng. Mater.* **2007**, *348*, 509.
[15] H. Castaneda, M. Galicia, *Front. Mater.* **2019**, *6*, 1.
[16] A. Ogawa, K. Takakur, N. Hirai, H. Kanematsu, D. Kuroda, T. Kougo, K. Sano, S. Terada, *Materials* **2020**, *13*, 923.
[17] W. Ding, W. Zhang, N. Mannalamkunnath, Z. Batang, B. Pei, R. Wang, L. Chen, A. Al-Suwailem, P. Qian, *Microb. Ecol.* **2019**, *77*, 406.
[18] A. Al-Jumaili, S. Alancherry, K. Bazaka, M. Jacob, *Materials* **2017**, *10*, 1066.
[19] V. Upadhyayula, V. Gadhamshetty, *Biotechnol. Adv.* **2010**, *28*, 802.

[20] T. Liu, Z. Guo, Z. Zeng, N. Guo, Y. Lei, T. Liu, S. Sun, X. Chang, Y. Yin, X. Wang, *ACS Appl. Mater. Interfaces* **2018**, *10*, 40317.
[21] M. Galicia, V. Valencia Goujon, M. Aguirre-Ramírez, H. Castaneda, *NACE-Int. Corros. Conf. Ser.* **2017**, *6*, 3786.
[22] W. Schwerdtfeger, *J. Res. NBS GO* **1958**, *153*, RP2833.
[23] W. Schwerdtfeger, *J. Res. Natl. Bur. Stand.* **1959**, *63C*, 1104.
[24] A. Bose, E. Gardel, C. Vidoudez, E. Parra, P. Girguis, *Nat. Commun.* **2014**, *5*, 3391.
[25] A. Kumar, L. Huan, P. Kavanangh, F. Barriere, L. Lapinsonniere, J. Lienhard, *Nat. Rev. Chem.* **2017**, *1*, 145.
[26] C. Palacios, J. Shadley, *Corrosion* **1991**, *47*, 122.
[27] F. Farelas, M. Galicia, B. Brown, S. Nesic, H. Castaneda, *Corros. Sci.* **2010**, *52*, 509.
[28] J. Jorcin, M. Orazem, N. Pebérè, B. Tribollet, *Electrochim. Acta* **2006**, *51*, 1473.
[29] Y. Huang, H. Shih, F. Mansfeld, *Mater. Corros.* **2010**, *61*, 302.
[30] L. Hongwei, G. Tingyue, A. Muhammad, Z. Guoan, L. Hongfang, *Corros. Sci.* **2017**, *114*, 102.
[31] S. Chongdar, G. Gunasekaran, P. Kumas, *Electrochim. Acta* **2005**, *50*, 4655.
[32] P. Kalnaowakul, D. Xu, A. Rodchanarowan, *ACS Appl. Biol. Mater.* **2020**, *3*, 2185.
[33] J. Phillips, N. van den Driessche, K. de Paepe, A. Prévoteau, J. A. Gralnick, B. Arendes, K. Rabaey, *Appl. Environ. Microbiol.* **2018**, *1*, 1.
[34] J. Huang, *Electrochim. Acta* **2018**, *281*, 170.
[35] S. E. Faidi, J. Scantlebury, P. Bullivant, N. Whittle, R. Savin, *Corros. Sci.* **1993**, *35*, 1319.
[36] P. SungMo, S. MinYoung, *J. Ind. Eng. Chem.* **2015**, *21*, 1258.
[37] S. Atmaca, K. Güli, R. Cícek, *Trans. J. Med. Sci.* **1998**, *28*, 595.
[38] N. Ohtsu, Y. Kakuchi, T. Ohtsuki, *Appl. Surf. Sci.* **2018**, *445*, 596.
[39] Y. Dai, T. Sun, Z. Zhang, Z. J. Zhang, J. Li, *Biointerphases* **2017**, *12*, 1.
[40] S. R. Taylor, E. Gileadi, *Corrosion* **1995**, *51*, 664.
[41] K. S. Salahuddin, A. ur Rahman, Tajuddin, A. Husen, *Nanoscale Res. Lett.* **2018**, *13*, 141.
[42] S. Kelly, C. Havrilla, T. Brady, K. Abramo, E. Levin, *Environ. Health Perspect.* **1998**, *106*, 375.
[43] T. Tong, C. Wilke, J. Wu, C. Binh, J. Kelly, J. Gaillard, *Environ. Sci. Technol.* **2015**, *49*, 8113.
[44] P. Sørensen, S. Kiil, K. Dam-Johansen, C. Weinell, *J. Coat. Technol. Res.* **2009**, *6*, 135.
[45] E. McMahon, R. Santucci, Jr., C. Glover, B. Kannan, Z. Walsh, J. Scully, *Front. Mater.* **2019**, *6*, 190.

How to cite this article: Calvillo Solís JJ, Galicia Garcia M. Electrochemical behavior of Zn-REP nanohybrid coatings during marine *Shewanella sp.* biofilm formation. *Materials and Corrosion*. 2021;1–15. https://doi.org/10.1002/maco.202011997